HOKKAIDO UNIVERSITY

Title	Deep Neural Networks Based End-to-End DOA Estimation System
Author(s)	Ando, Daniel Akira; Kase, Yuya; Nishimura, Toshihiko et al.
Citation	IEICE transactions on communications, E106B(12), 1350-1362 https://doi.org/10.1587/transcom.2023CEP0006
Issue Date	2023-12-01
Doc URL	https://hdl.handle.net/2115/91226
Rights	copyright©2023 IEICE
Type	journal article
File Information	E106.B_2023CEP0006.pdf

Hokkaido University Collection of Scholarly and Academic Papers : HUSCAP

IEICE TRANS. COMMUN., VOL.E106–B, NO.12 DECEMBER 2023

PAPER Special Section on Emerging Communication Technologies in Conjunction with Main Topics of ICETC 2022

Deep Neural Networks Based End-to-End DOA Estimation System*

Daniel Akira ANDO[†a)], ***Student Member***, **Yuya KASE**[†], ***Nonmember***, **Toshihiko NISHIMURA**[†], ***Senior Member***, **Takanori SATO**[†], ***Member***, **Takeo OHGANE**[†b)], **Yasutaka OGAWA**[†], ***Fellows***, ***and*** **Junichiro HAGIWARA**[†], ***Member***

SUMMARY Direction of arrival (DOA) estimation is an antenna array signal processing technique used in, for instance, radar and sonar systems, source localization, and channel state information retrieval. As new applications and use cases appear with the development of next generation mobile communications systems, DOA estimation performance must be continually increased in order to support the nonstop growing demand for wireless technologies. In previous works, we verified that a deep neural network (DNN) trained offline is a strong candidate tool with the promise of achieving great on-grid DOA estimation performance, even compared to traditional algorithms. In this paper, we propose new techniques for further DOA estimation accuracy enhancement incorporating signal-to-noise ratio (SNR) prediction and an end-to-end DOA estimation system, which consists of three components: source number estimator, DOA angular spectrum grid estimator, and DOA detector. Here, we expand the performance of the DOA detector and angular spectrum estimator, and present a new solution for source number estimation based on DNN with very simple design. The proposed DNN system applied with said enhancement techniques has shown great estimation performance regarding the success rate metric for the case of two radio wave sources although not fully satisfactory results are obtained for the case of three sources.

key words: *antenna array, DOA estimation, SNR estimation, source number estimation, deep neural network*

1. Introduction

Several practical applications in the field of wireless technologies such as radar systems, source localization, and channel state information retrieval have in common the necessity for predicting the direction of arrival (DOA) of incoming radio waves. With the further development of the current fifth-generation (5G) mobile system, and ongoing research on the sixth-generation (6G) system, an enormous expansion of use case ideas is expected [1]. Therefore, it is vital that the existing technologies, including DOA estimation techniques, remain supporting this envisioned communications system architecture. In other words, more accurate and computationally less complex solutions will be greatly demanded.

Various techniques have been developed to estimate the DOA of radio waves, such as the super-resolution multiple signal classification (MUSIC) algorithm [2], and its extended version, root-MUSIC [3]. MUSIC is classified as a subspace-based technique, as the spectral decomposition of the correlation matrix of the antenna array received signal is required. Root-MUSIC, being an extension of MUSIC, achieves better estimation performance [3]. However, matrix eigendecomposition, a computationally complex procedure, is required for both algorithms.

Given the sparse radio environment inherent to most DOA estimation problems, compressed sensing techniques have also been heavily studied [4], [5]. These are a group of methods whose purpose is to obtain a unique solution from an underdetermined linear system taking advantage of the sparsity propriety of the true solution. Solving these linear systems is done by minimization of an l_p-norm constraint ($0 \leq p \leq 1$), where methods such as half-quadratic regularization (HQR) [6] usually assume $0 < p < 1$. These and many other methods are attractive due to their benefit of requiring a smaller number of snapshots and their ability to deal with coherent signals.

Recently, artificial intelligence techniques, especially deep learning, applied to the field of communication systems has become a trending research topic [7]. Although offline training of deep neural networks (DNN) is computationally heavy, once it is over, it can be easily applied to that specific situation which it was trained for with considerably low complexity, since only matrix multiplication is done. In fact, the applicability of DNNs in the DOA estimation problem has been reported in several studies, such as [8]–[11]. In [8], a framework for end-to-end channel and DOA estimation in the context of massive multiple-input multiple-output (massive MIMO) is proposed. In [9], a combination of a detection and DOA estimation network, which reduces the training-set size and makes it possible to train several DNNs corresponding to different position sectors, is presented. In [10], a low-complexity DOA estimation technique for hybrid MIMO systems with uniform circular array at a base station is presented. In [11], a DOA estimation system which is robust to array imperfections and consists of a multi-task autoencoder and a series of parallel multi-layer classifiers is explained.

One of the main goals of this paper is the proposal of an end-to-end DOA estimation system. It consists of three components, whose schematics are shown in Fig. 1: Source number estimator, DOA angular spectrum grid estimator,

Manuscript received February 26, 2023.
Manuscript revised June 12, 2023.
Manuscript publicized September 11, 2023.

[†]The authors are with the Graduate School/Faculty of Information Science & Technology, Hokkaido University, Sapporo-shi, 060-0814 Japan.

*A part of this paper was presented at Wireless Personal Multimedia Communications (WPMC 2022) [18].

a) E-mail: dakiraando@m-icl.ist.hokudai.ac.jp
b) E-mail: ohgane@m-icl.ist.hokudai.ac.jp

DOI: 10.1587/transcom.2023CEP0006

Copyright © 2023 The Institute of Electronics, Information and Communication Engineers

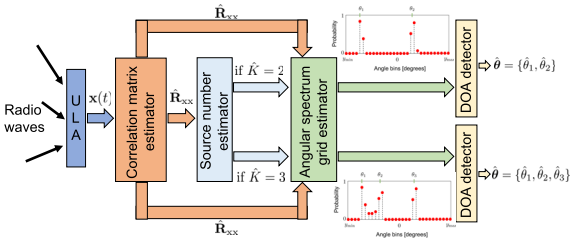

Fig. 1 Proposed system schematics where $\hat{K}$ and $\hat{\theta}$ denote estimated values of the number of sources and DOAs, respectively.

and DOA detector. The correlation matrix of the signals received at the antenna array is used as input data to the first two components in order to estimate the respective quantities, that is, source number and angular spectrum grid. In the first component, the number of radio waves $\hat{K}$ is predicted with an offline trained DNN. Note that, this mainly being a preliminary study, we consider only 2 and 3 sources. In air-to-air emitter location or radar systems, 2 or 3 flying objects in the field of view of an antenna array is an imaginable scenario as stated in [13]. Additionally, as it was verified in [14], the average number of subpaths, or multipaths, — whose DOAs estimation is necessary — at sub-terahertz and line-of-sight environments of 140 GHz is significantly small, e.g. mostly ranging between 2 and 5, compared to 5G system frequency bands. Therefore, our 2 and 3 sources consideration is not only realistic in airborne radar applications based on [13], but also it is a first step towards the goal of radio propagation measurements at sub-terahertz bands [14]. Yet, as it will be detailed later, simply expanding our setting from 2 sources [16], [17] to 3 brings new challenges that need to be addressed prior to fully leveraging DNNs as methods for DOA estimation. Next, in the second component, the angular spectrum grid is estimated with an also offline trained DNN. Finally, in the last component, a DOA detection algorithm is applied onto this angular spectrum grid in order to extract the DOA information. Moreover, we design new strategies for further enhancement of the DOA detector and spectrum estimator accuracy. Computer simulations will confirm that they overall manage to surpass not only our past methods but also root-MUSIC.

In summary, our contributions in this work are: (1) proposal of a new and more precise DOA detection algorithm, (2) development of new methods for enhanced DOA angular spectrum grid estimator performance, (3) design of new SNR estimation schemes incorporated in the new DOA methods and its detailed verification when used within the proposed end-to-end system, (4) a powerful DNN with very simple design specific for source number estimation, and (5) evaluation of DOA estimation performance by adding a regularization l_p-norm term to the DNN loss function. A convolutional neural network pooling layer with l_p-norm is presented in [12], but to the authors' knowledge, a loss function constrained by this norm has not yet being reported. Moreover, all the above discussion is thoroughly conducted based on computer simulations with the aid of the Tensorflow framework [15].

The reminder of this paper is structured as follows. The antenna array model is explained in Sect. 2. Our previous work results on the DNN design and training for DOA estimation are given in Sect. 3. The newly designed DOA detection algorithm for the DOA detector module of the proposed system is detailed in Sect. 4. Two new approaches for further enhancement of DOA angular spectrum grid estimation are fully explained in Sect. 5. It can also be found therein detailing about two different schemes for SNR estimation from the received signal correlation matrix, which are needed for the said DOA enhancement approaches. The simple-design DNN for the source number estimator is explained in Sect. 6. Finally, all computer simulation results and discussion on the viability of the proposed end-to-end system are given in Sect. 7. Moreover, analysis of adding a regularization l_p-norm term to the DNN loss function is also briefly presented in Sect. 8. Lastly, in Sect. 9 our results are summarized.

2. Antenna Array Model

Throughout this study, we consider a uniform linear array (ULA) with L omnidirectional antennas. They are placed at half-wavelength spacing from each other and no mutual coupling is assumed. K sources located in the ULA far-field region emit narrowband radio waves that are impinging on the ULA at angles $\boldsymbol{\theta}[\text{rad}] = [\theta_1, \ldots, \theta_K]^T$, where $[\cdot]^T$ indicates the transpose operator. In addition, it is assumed that they are at least 1° mutually separated. As a result, the baseband received signal $\mathbf{x}(t) \in \mathbb{C}^{L\times 1}$ at the ULA can be modeled by

$$\mathbf{x}(t) = \mathbf{A}(\boldsymbol{\theta})\mathbf{s}(t) + \mathbf{z}(t), \tag{1}$$

where $\mathbf{s}(t) \in \mathbb{C}^{K\times 1}$ is the vector containing the incident radio waves complex amplitudes, $\mathbf{z}(t) \in \mathbb{C}^{L\times 1}$ is the additive white Gaussian noise vector following a circular complex Gaussian distribution $\mathbf{z}(t) \sim \mathcal{CN}(0, \sigma^2\mathbf{I}_L)$ with zero mean and variance σ^2, where $\mathbf{I}_L$ represents a L-dimensional identity matrix, and $\mathbf{A}(\boldsymbol{\theta})$ is the steering matrix, which accounts for the relative delay corresponding to path length difference of the incident waves on each ULA element and is described as

$$\mathbf{A}(\boldsymbol{\theta}) = \begin{bmatrix} 1 & \cdots & 1 \\ e^{-j\pi\sin\theta_1} & \cdots & e^{-j\pi\sin\theta_K} \\ e^{-j\pi 2\sin\theta_1} & \cdots & e^{-j\pi 2\sin\theta_K} \\ \vdots & \ddots & \vdots \\ e^{-j\pi(L-1)\sin\theta_1} & \cdots & e^{-j\pi(L-1)\sin\theta_K} \end{bmatrix}. \tag{2}$$

Another assumption in this work is that the incident radio waves are non-coherent and are transmitted with equal power normalized to one.

Traditionally, the received signal correlation matrix $\mathbf{R}_{xx}$ is used for DOA estimation. However, due to the impossibility of its direct calculation, here the correlation matrix estimated by N snapshots $\hat{\mathbf{R}}_{xx}$ is used instead:

$$\hat{\mathbf{R}}_{xx} = \frac{1}{N}\sum_{n=1}^{N}\mathbf{x}(t_n)\mathbf{x}(t_n)^H, \tag{3}$$

where $\mathbf{x}(t_n)$ represents the nth snapshot taken from the received signal, and $(\cdot)^H$ is the conjugate transpose operator. As it was mentioned in Sect. 1, $\hat{\mathbf{R}}_{xx}$ is used as input data to the first two estimators in our proposed system.

3. Authors' Previous Work

In [16], [17] a DOA estimation scheme based solely on deep neural networks was proposed. As a primary assessment of its performance, just two incoming radio waves and a rather small-sized array with five antenna elements were considered. Here, we briefly explain the DNN structure, and its input-output data generation, which are equally used throughout this paper. For a more detailed explanation, refer to [16].

A traditional feed-forward neural network consisting of one input layer, one output layer and an arbitrary number of hidden layers is used (Fig. 2). Here, batch normalization, a powerful regularizer normally used as an improvement of the overall stability of the learning process, is also used in all layers [21]. As it can be seen, the overall DNN structure is kept simple, yet very accurate results were previously achieved. The next step of our discussion is the design of each layer, starting from the input and output layers respectively.

First, the estimated correlation matrix $\hat{\mathbf{R}}_{xx}$ must be transformed to a vector and this must be converted to the real domain. This step in preparing the DNN input data is necessary due to the fact that inputs to fully connected DNNs are one-dimensional, and forward and backpropagation computation is defined in the real domain. Since $\hat{\mathbf{R}}_{xx}$ is a Hermitian matrix, it can be written as in (4). A proper input vector $\mathbf{u}$ to the DNN can then be generated as follows: first we arrange the diagonal elements of (4) on the first input vector entries; next, we only use the lower triangular elements, by taking each element real $\Re(\cdot)$ and imaginary $\Im(\cdot)$ part column by column and from left to right and arranging it in the remaining space of the input vector (See (5)). This is possible because the lower triangular elements are simply the complex conjugate of the upper triangular elements.

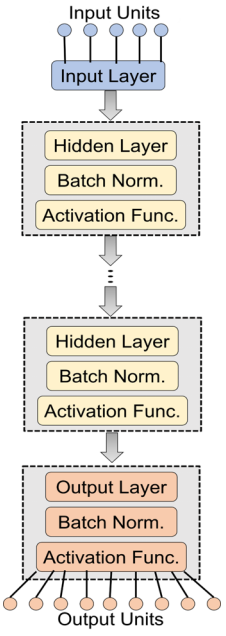

Fig. 2 DNN structure with input, hidden, and output layers.

$$\hat{\mathbf{R}}_{xx} = \begin{bmatrix} r_{11} & r_{21}^* & \cdots & r_{L1}^* \\ r_{21} & r_{22} & \cdots & r_{L2}^* \\ \vdots & \vdots & \ddots & \vdots \\ r_{L1} & r_{L2} & \cdots & r_{LL} \end{bmatrix} \tag{4}$$

$$\mathbf{u} = [r_{11},\ldots,r_{LL},\Re(r_{21}),\Im(r_{21}),\ldots,\Re(r_{L1}), \Im(r_{L1}),\ldots,\Re(r_{L(L-1)}),\Im(r_{L(L-1)})]^T. \tag{5}$$

The resulting input vector $\mathbf{u}$ has now L^2 components, each corresponding to one unit of the DNN input layer.

In this work, we consider that the DOA angle spectrum is discretized in angle bins, each corresponding to one output layer unit. When they range from $y_{\min}$ to $y_{\max}$ in steps of y_{step}, then the total amount of angle bins, and thus the total number of output layer units becomes $\{(y_{\max}-y_{\min})/y_{\text{step}}+1\}$. As it is shown in (6) below, each bin describes the probability of radio wave incidence onto it. In case of radio wave presence, an output 1 is expected, and 0 otherwise.

$$y_j = \begin{cases} 1 & \text{if wave is incident onto the } j\text{th bin} \\ 0 & \text{otherwise} \end{cases}. \tag{6}$$

Finally the training, validation, and test datasets can be reproduced by the method described above. The DNN weights are updated according to the optimizer algorithm Adam [22] with respect to the gradient calculated from the loss function, the mean square error (MSE).

Following our previous studies, the success rate (here also named probability of correct DOA estimation) is the metric used for verifying 1) the learning progress during the validation phase and 2) the DOA estimation performance during the testing phase. A DOA prediction $\hat{\boldsymbol{\theta}} = [\hat{\theta}_1,\ldots,\hat{\theta}_K]^T$ in degrees is counted as a success solely when all DOAs $\boldsymbol{\theta} = [\theta_1,\ldots,\theta_K]^T$ in a dataset sample are correctly detected:

$$\text{Success} \iff |\theta_j - \hat{\theta}_j| \le \mu, \forall j \in \{1,\ldots,K\}, \tag{7}$$

where μ is the estimation tolerance, considered in this study to be 0.5° (prediction to the closest bin). In an effort to avoid overfitting, the DNN weights corresponding to the best success rate are saved for further use at the test phase. Yet, note that these are not necessarily optimal in terms of the root mean squared error (RMSE), which is another metric mainly used during the test phase, and can be expressed as:

$$\text{RMSE} = \sqrt{\frac{1}{KN_t}\sum_{k=1}^{K}\sum_{n=1}^{N_t}\left(\hat{\theta}_k^{(n)} - \theta_k^{(n)}\right)^2}, \tag{8}$$

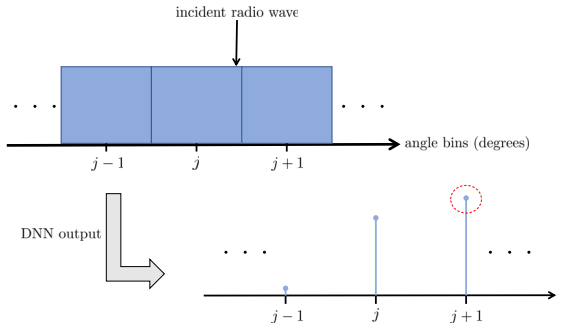

Fig. 3 Consequence of radio waves incident on the angle bin border. The $j+1$ bin is mistakenly detected as the true DOA.

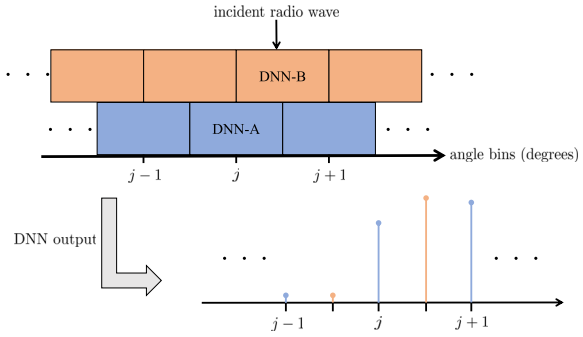

Fig. 4 Visualization of staggered DNNs. After combining both DNN-A and DNN-B grids, correct DOA detection is made possible.

where N_t is the total number of test samples.

In [16], [17], we demonstrated that this DNN design achieved good performance in comparison with the traditional root-MUSIC and the compressed sensing technique HQR. However, decline in DOA detection accuracy is heavily influenced by radio waves impinging onto the angle bin border, which causes neighboring bins to be concurrently excited. This then blinds the true DOA bin during detection (see Fig. 3). An effective approach proposed in [17] is to stack up on top of a main DNN (called DNN-A) a second one (DNN-B), whose output grid had been shifted by half DNN-A grid spacing, ranging from $-60.5°$ to $+60.5°$. This method was then named staggered DNN, and it is shown in Fig. 4. A standard peak search algorithm generally succeeded in correctly detecting the DOA, however a more accurate DOA detection algorithm is developed and presented in Sect. 4.

4. DOA Detector

In [16], [17], DOA detection from the DNN output spectrum was carried out with a method here called "Largest Search", where the angle bins corresponding to the largest K angle spectrum values were simply chosen as the DOA estimates. However, specially when $K = 3$, "Largest Search" fails to provide sufficient detection accuracy, due to spurious DNN output values in the neighborhood of the bins corresponding to true DOAs. Moreover, at times these spurious outputs are even larger than the true bin values (see how the probability of incident radio wave at the spurious bin $-41°$ is higher than both bins $-46°$ and $-45°$ in Fig. 5, overshadowing them during DOA detection with "Largest Search"). The peak search algorithm, though managing to solve the case presented here, has also not proven to be a viable solution overall. For this reason, we propose a new DOA detection algorithm, here named "Neighbors Average". The idea is to first search for all largely enough excited bins (here we consider all bins with probability of incident radio wave higher than 0.2), and then averaging out mutually near bins. For instance, as it is shown in Fig. 5(b), the estimated DOAs are $-45.5°$ and $-41.5°$ within the considered angle bin window.

5. Performance Improvement in Angular Spectrum Grid Estimation

The other objective of this paper is to further enhance DOA estimation performance. Therefore, here we present two new angular spectrum grid estimator approaches: "SNR-based switching DNN" and "SNR-based Switching Staggered DNN".

When training the DNN, we use datasets generated at randomly variable or at different individual SNRs. We verified that a DNN, which had been offline trained at a specific SNR and subsequently tested at this SNR, shows the greatest DOA estimation accuracy. For instance, a DNN offline trained with a 5 dB dataset and then tested at it presents better performance than any other DNN offline trained with a dataset generated at any SNR other than 5 dB. This result led us to the development of the strategy here named "SNR-based Switching DNN", where a new module, SNR estimator, is introduced to the schematics of Fig. 1.

Now we detail each proposed approach, starting from the SNR estimator design.

5.1 SNR Estimator

Here we consider only discrete values of SNR: 0, 5, 10, 15, and 30 dB[†]. The main idea is to develop a technique able to detect the SNR from the estimated correlation matrix $\hat{\mathbf{R}}_{xx}$. Therefore, two different approaches are presented and compared: DNN-based and regression-based SNR estimation.

(a) DNN-based Estimation

The DNN considered for SNR estimation follows the same layout as shown in Fig. 2. This must be trained using an input dataset that was generated at a fixed number of sources K. Therefore, in this study, we must train two DNNs: one with a dataset generated at $K = 2$ and another at $K = 3$ (See the description of the proposed system in Sect. 1). While we feed the same input data (the estimated correlation matrix $\hat{\mathbf{R}}_{xx}$) to this DNN, the output must be fitted to this problem

[†]It was verified that the DNN trained at 30 dB provides better DOA detection performance at 20 and 25 dB. Therefore, complexity reduction is achieved as training of DNNs at these SNRs becomes unnecessary.

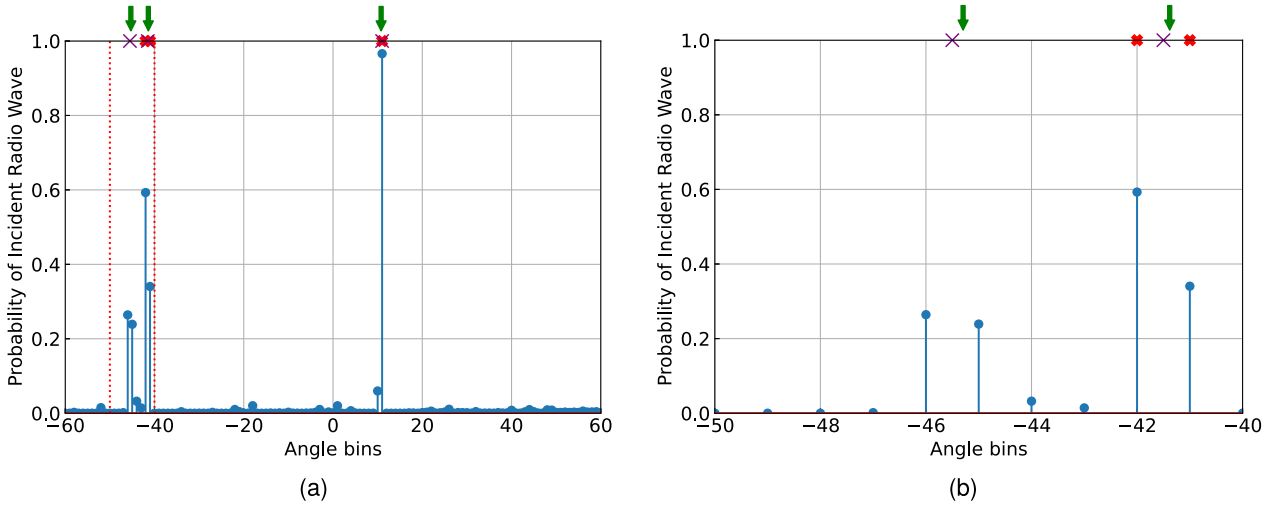

Fig. 5 (a) DNN output angle spectrum for a DNN trained offline at 30 dB and tested at 30 dB. Green arrows represent true DOAs, red thick crosses represent estimated DOAs by "Largest Search", and purple thin crosses represent estimated DOAs by "Neighbors Average". (b) Zoomed-in plot of (a) within the range $[-50°, -40°]$, highlighted by the red dotted rectangle.

accordingly. Since here one SNR value (one label) should be selected from a set thereof (different labels), this turns into a multilabel classification problem. For this reason, the appropriate loss function becomes the categorical cross-entropy.

(b) Regression-based Estimation

It was verified through computer simulations that the previous strategy does not provide very high estimation accuracy specially when $K = 3$. In an attempt to increase this accuracy, here we propose a second approach for SNR estimation.

We observed that the SNR in dB and $-\log(\lambda_s)$ are linearly correlated, where λ_s represents the smallest eigenvalue of the correlation matrix $\hat{\mathbf{R}}_{xx}$. In order to obtain a prediction function for the SNR based on $-\log(\lambda_s)$ as input, we train a regression model based on the ordinary least squares method. Since both our input and output data are one-dimensional, the linear function that approximates the desired prediction function has only two coefficients: the y-intercept and the slope. These can be calculated by minimizing the residual sum of squares between the observed and the predicted SNRs. After fitting the training dataset to this model, the following SNR prediction function when $K = 2$ is obtained:

$$\text{SNR (dB)} = -0.99644 + 9.98865(-\log(\lambda_s)). \quad (9)$$

When $K = 3$:

$$\text{SNR (dB)} = -0.72178 + 10.01046(-\log(\lambda_s)). \quad (10)$$

Next, the closest value within the set $\{0, 5, 10, 15, 30\}$ to the SNR predicted by (9) and (10) should be chosen as the final SNR estimate $\hat{\gamma}$.

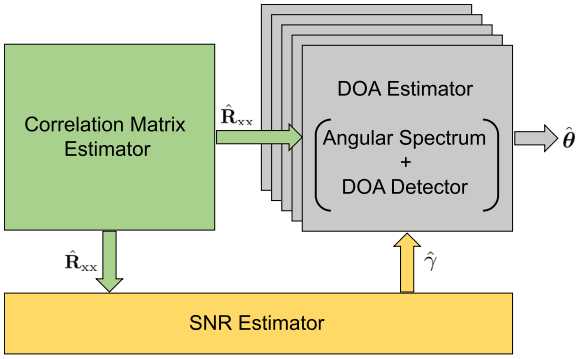

Fig. 6 Schematics of the proposed SNR-based Switching DNN.

5.2 Angular Spectrum Grid Estimator

(a) SNR-based Switching DNN

Leveraging the result explained in the beginning of this section, where DNN performance is best at a specific SNR when it had been trained at this SNR, here we propose a technique consisting of the following steps (Fig. 6): first, estimate SNR from the estimated correlation matrix; second, select the appropriate DNN (which was previously trained offline at this estimated SNR); third, estimate the angular spectrum grid with the selected DNN. By doing so, the most appropriate DNN is allowed to work at the environment for which it was trained.

(b) SNR-based Switching Staggered DNN

Our second proposed scheme is simply the combination of SNR-based Switching DNN with the strategy previously proposed in [17], Staggered DNN. The same issue concerning

incident radio waves onto the angle grid border vicinity was also confirmed for the other SNR values. Therefore it is natural to use the Staggered DNN method in order to overcome it again. Later simulation results will show that this strategy is indeed the one achieving best results overall.

First, five pairs of DNN-A and DNN-B must be trained offline in advance for each considered SNR value (0, 5, 10, 15, and 30 dB). Next, the appropriate DNN pair is selected based on the SNR estimated from the correlation matrix. Then, the combined angular spectrum is produced by the DNN-A and B pairs, and finally the DOA detection algorithm is applied on this spectrum in order to estimate the DOA. The schematics is very similar to that of Fig. 6, with only the addition of DNN-Bs within the DOA estimator module. Moreover, all DNN-As and DNN-Bs are designed with the same architecture (number of hidden layers and units per layer) as an effort to simplify the processing, since only shifting of optimized model weights between selected DNNs is done.

6. Source Number Estimator

The DNN specialized in source number estimation also has as input data the vectorized form of the correlation matrix (see (5)). As explained in Sect. 1, only 2 or 3 radio wave sources are assumed. For this reason, the label data should be in one-hot representation, where, for instance, $[0, 1]$ corresponds to 2, and $[1, 0]$ to 3 sources.

The first module of our proposed system is the source number estimator. Consequently, this DNN must guarantee enough generality so as to correctly predict the number of incoming radio waves at different SNRs. We generate the datasets by sampling the SNR from a uniform distribution from 0 to 30 dB, and randomly shifting the number of sources between 2 and 3 at each sample. The remaining parameters are kept unchanged as it is detailed in Table 2.

The size of this DNN architecture is relatively small, as there are only two possible classes in this classification problem. The input layer has L^2 units, the output layer has 2 units, and there are 2 hidden layers with 50 units each. The hidden layers and the output layers activation functions are ReLU and Softmax, respectively. The loss function to be minimized is the categorical cross-entropy. Batch size is 128, and the total number of epochs is 10. The remaining hyperparameters are the same as those for the DOA estimator.

After the conclusion of the training of this DNN, we have obtained the prediction success rates given in Table 1 at the test phase. Roughly 99% of source number estimation accuracy has been achieved for all SNRs.

7. Simulation Results

The performance evaluation of all components and ultimately the proposed end-to-end system is now described here. Since there are in total 4 components that need offline training in advance (source number, DNN and regression-based SNR, and angle spectrum grid estimators), 4 training and validation datasets are generated. The peculiarities of these datasets will be discussed below in their corresponding subsection. As previously mentioned in Sect. 3, two metrics are used here for overall performance evaluation: probability of correct DOA estimation and RMSE. Their importance relies on the type of application. The probability of correct DOA estimation should be of more relevance in such cases where correct estimation of all DOAs within one sample is vital. On the other hand, in such cases where average precision is more important than occasional detection error within a sample, RMSE should be mostly considered. Nevertheless, as the RMSE is very sensitive to outliers, other metrics should be regarded concurrently, such as the absolute error median. This is however left as future work.

Table 1 Source number estimator performance for each SNR (in %).

		SNR (dB)						
		0	5	10	15	20	25	30
K	2	99.21	99.87	99.94	99.95	99.96	99.95	99.95
	3	99.87	99.84	99.86	99.87	99.87	99.86	99.85

Table 2 Parameters for data generation.

Number of antenna elements L	5
Number of incident radio waves K	2, 3
Direction of arrival angles $\boldsymbol{\theta}$	random from −60.5° to +60.5°
Number of snapshots N	100
Number of training data samples	250,000
Number of validation data samples	10,000
Number of test data samples N_t	150,000

7.1 DOA Detector

In order to verify the performance of the proposed DOA detector "Neighbors Average" (Sect. 4), we have tested it with two different angle spectrum grid estimators: the single DNN and Staggered DNN (both previously proposed in [16], [17] and explained in Sect. 3), while comparing it with the previous detectors "Largest Search" and conventional peak search, respectively. These DNNs, whose training parameters can be seen in Table 3, were offline trained with a dataset generated according to the parameters listed in Table 2, where the SNR was set to 30 dB. Then, test data samples are equally generated at other SNRs, i.e. there are 150,000 samples for each SNR value.

As it can be seen in Fig. 7, we have verified that, compared to "Largest Search" applied to single DNN output spectrum, DOA detection accuracy has improved considerably when "Neighbors Average" is used. In addition, specially in terms of RMSE, "Neighbors Average" has proven

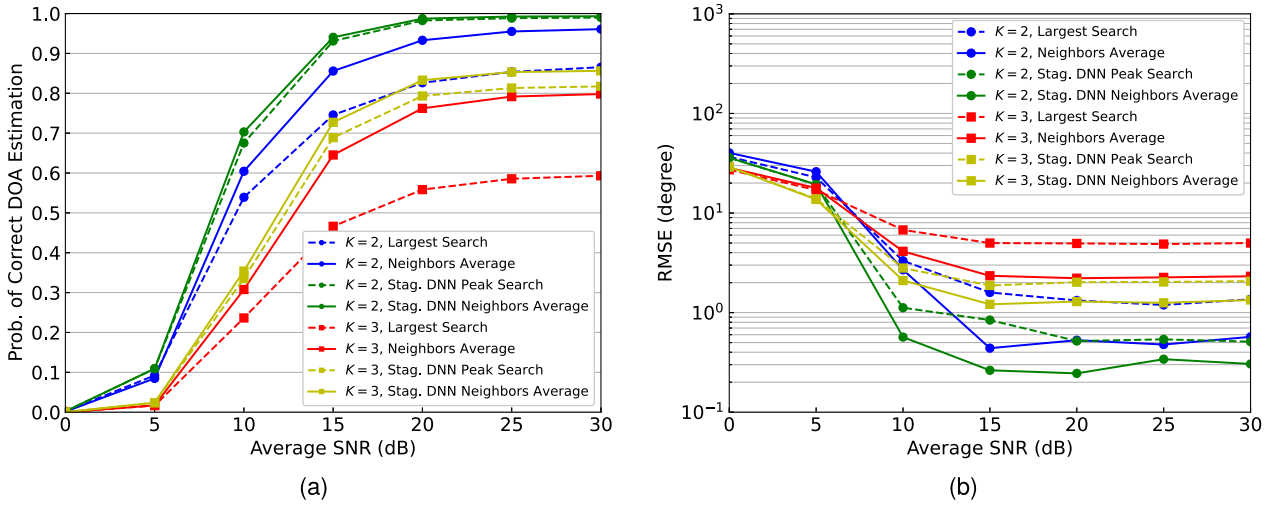

Fig. 7 Estimation accuracy improvement by the proposed technique named "Neighbors Average". (a) Probability of correct DOA estimation. (b) RMSE.

Table 3 Parameters for DNN training.

Input layer units	25
Hidden layers	4
Units per hidden layer	DNN-A: 363 DNN-B: 366
Output layer units	DNN-A: 121 DNN-B: 122
Hidden layers activation function	ReLU
Output layer activation function	Sigmoid
Loss function	MSE
Optimizer	Adam
Batch size	256
Number of epochs	300

to be more accurate than peak search applied to Staggered DNN output spectrum.

It was also noticed that this proposed DOA detection method does not cover well certain situations, such as the case of narrowly incident radio waves. Averaging out such bins corresponding to narrow radio waves leads to incorrect DOA estimation, as one DOA had been potentially ignored by the algorithm. Therefore, further investigation for mitigation techniques is necessary.

Another possibility to detect the DOA is to train a machine learning model (such as another DNN), in such a way that the bin probabilities could provide a better guidance to where the DOAs are within the angle spectrum grid. However, this option is costly, since the training of one more model is needed. Therefore, we believe that, although possibly not the most optimal technique, "Neighbors Average" provides sufficient accuracy at low computational cost. In all subsequent numerical simulations "Neighbors Average" will be the technique used for the DOA estimator module.

7.2 SNR Estimator

Here we test both our proposed SNR estimators: DNN-based and regression-based (Sect. 5.1). The training, validation, and test data samples for the DNN-based estimator are generated according to the parameters in Table 2. While the input data samples follow the same format as shown in (5), the output data samples are in one-hot representation, where each label corresponds to the SNR class within the set {0, 5, 10, 15, 30} dB. In order to verify the validity of this scheme, we trained and tested DNNs with varying hidden layers (2, 3, 4, and 5) and units thereof (121, 182, 242, 303, 363, 424, 484, 545, and 605), totaling 36 DNNs. Parameters for the training phase are the same as those in Table 3, with the exception that the number of epochs was raised to 1,000 and the number of test data samples was reduced to 50,000. When the training and test datasets correspond to $K = 2$, we concluded that the most optimal architecture was: 3 hidden layers and 182 units per hidden layer. The achieved SNR estimation success rate was approximately 80%, where the error tolerance is considered to be 2.5 dB.

The training, validation, and test data samples for the regression-based estimator are also generated according to the parameters in Table 2. In order to generate the input data samples to the linear regression model, $-\log(\lambda_s)$ is calculated for each sample of the estimated correlation matrix $\hat{\mathbf{R}}_{xx}$. As for the output, the SNR at which each corresponding input data was generated is used as the output data samples. We verified that this second approach achieves approximately 94% estimation success rate with the same test dataset as that of the DNN-based estimator when $K = 2$. This promptly shows that the regression-based approach is superior.

The prediction accuracy comparison between both methods can be seen in Fig. 8, where only 5,000 samples of the test dataset were used for better visualization. From

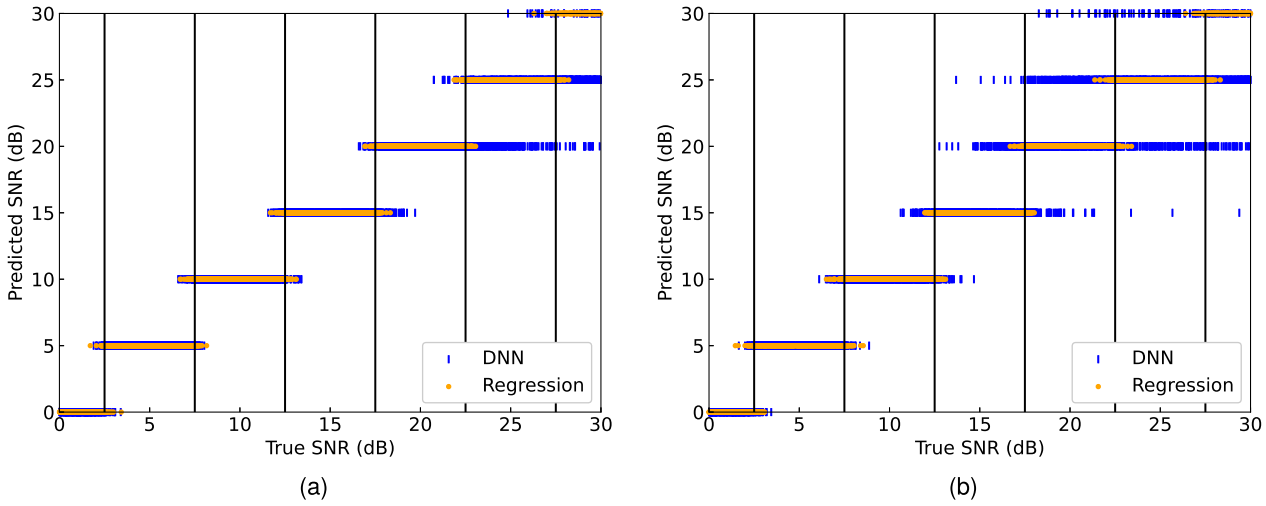

Fig. 8 SNR estimation performance comparison between DNN and linear regression obtained from 5,000 samples. The abscissa label "True SNR" corresponds to the SNR manually set during simulation. (a) $K = 2$. (b) $K = 3$.

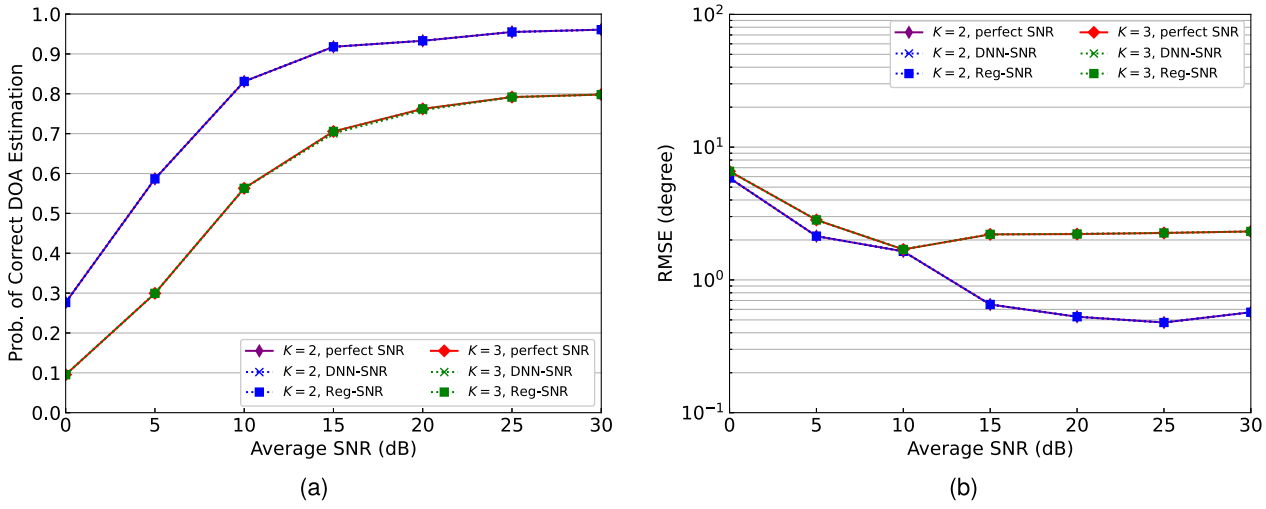

Fig. 9 DOA detection accuracy comparison with the "SNR-based Switching DNN" method when the SNR estimator module is perfect, DNN-based, and regression-based, for the cases $K = 2$ and 3. (a) Probability of correct DOA estimation. (b) RMSE.

this figure it is also noticeable how much better the performance is when estimating with linear regression, specially for higher SNR and for both values of source number K. Yet, as it will be shown next, this regression-based estimation is not necessarily the only viable option between the two.

7.3 Angular Spectrum Grid Estimator

Here we investigate the performance of the 2 proposed angle spectrum grid estimators "SNR-based Switching DNN" and "SNR-based Switching Staggered DNN". The training, validation, and test datasets are reproduced following the parameters listed in Table 2. Although these datasets were randomly generated for this work, thorough verification by means of resampling methods [19], [20], such as K-fold cross validation, needs to be addressed in the future study. In addition, the DNN training parameters are summarized in Table 3.

First, we verify the influence of perfect and imperfect SNR estimation over the performance of the proposed "SNR-based Switching DNN", using the success rate and RMSE metrics explained in Sect. 3. From Fig. 9, surprisingly the probability of correct DOA is virtually unchanged, whether using one approach or the other. Even compared to the ideal case of perfect SNR estimation, no significant changes are seen. These results suggest that, even when imperfect SNR prediction is carried out, the selected DNNs for DOA estimation maintain their robustness. In the upcoming discussions, we have opted to use the regression approach for its low complexity under the considered array dimension in this paper.

Next, we compare the performance of the 2 proposed

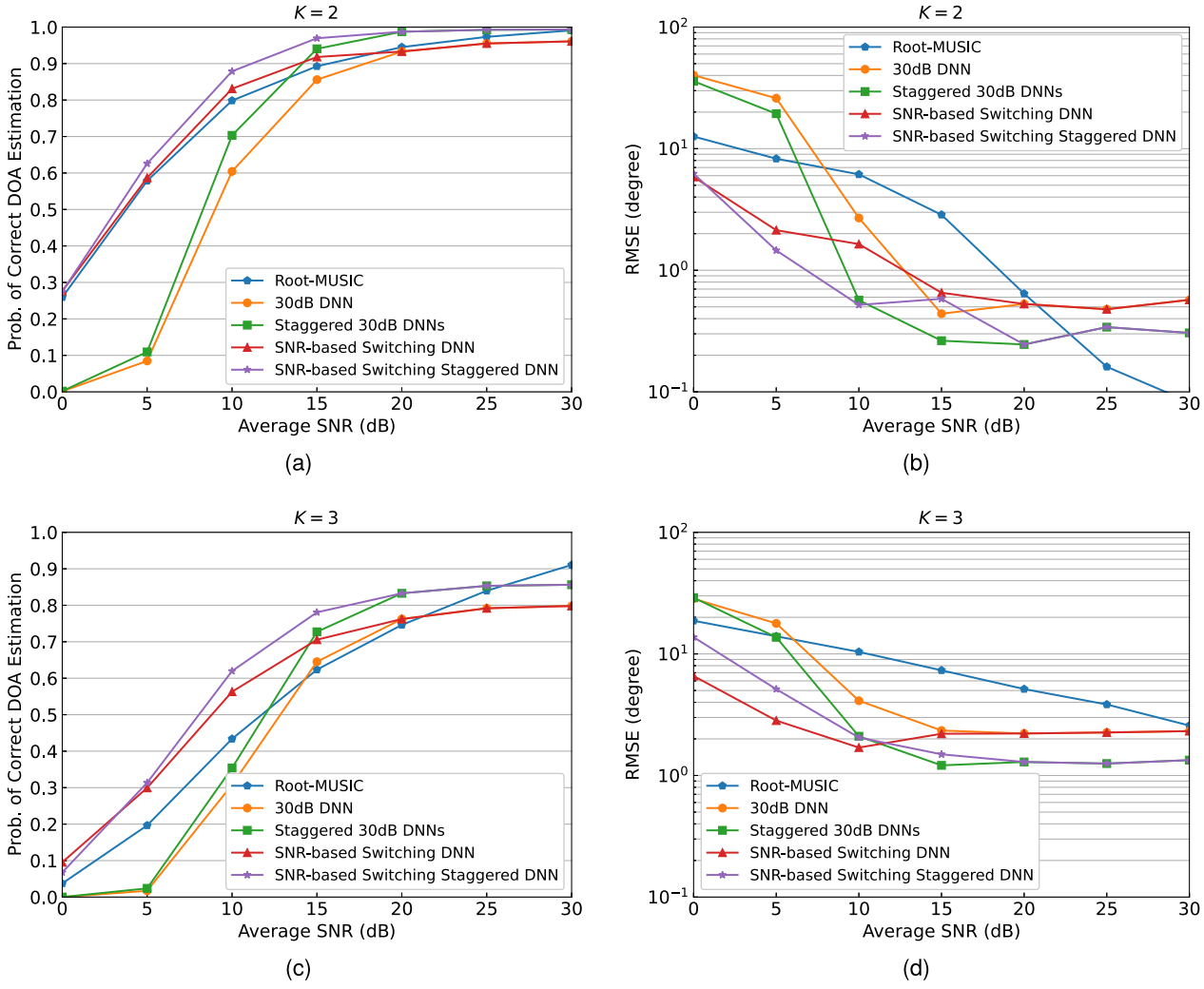

Fig. 10 Metrics comparison from same test dataset between Root-MUSIC and the two previous and two newly proposed DOA estimation methods. "30 dB DNN" corresponds to a DNN trained with a dataset generated from 30 dB data; "30 dB Staggered DNN" corresponds to DNN-A and DNN-B trained with a dataset generated from 30 dB data; "SNR-based Switching DNN" corresponds to the method of selecting the appropriate DNN based on SNR estimation; "SNR-based Switching Staggered DNN" is the method combining SNR-based Switching and Staggered DNNs. (a) Probability of correct DOA estimation when $K = 2$. (b) RMSE when $K = 2$. (c) Probability of correct DOA estimation when $K = 3$. (d) RMSE when $K = 3$.

methods "SNR-based Switching DNN" and "SNR-based Switching Staggered DNN" with root-MUSIC and our 2 previous techniques "30 dB DNN" and "30 dB Staggered DNN" [16], [17]. "30 dB DNN" corresponds to the DNN trained offline with a 30 dB dataset and "Neighbors Average" (Sect. 4) as the DOA detection algorithm; "30 dB Staggered DNNs" corresponds to both DNN-A and DNN-B trained offline with a 30 dB dataset and also "Neighbors Average" as the DOA detection algorithm; The results can be seen in Fig. 10, where we use the same test dataset for all methods.

When the proposed approaches are contrasted with root-MUSIC for the case $K = 2$, it can be seen that "SNR-based Switching Staggered DNN" demonstrates the best performance in terms of success rate (Fig. 10(a)). While both proposed methods "SNR-based Switching DNN" and "SNR-based Switching Staggered DNN" showed the best RMSE performance at lower SNRs, none fully stands out at higher ones. All curves reach a floor at higher SNRs, thus losing against root-MUSIC. However, this outcome was expected due to the limitation that our DNN solutions are classified as on-grid DOA estimation, so quantization error is inevitable.

Observing first the success rate for the case $K = 3$ (Fig. 10(c)) both "SNR-based Switching DNN" and "SNR-based Switching Staggered DNN" achieve better precision than root-MUSIC until 20 dB. At 30 dB, root-MUSIC surpasses all methods. Contrarily, regarding the RMSE (Fig. 10(d)), root-MUSIC presents much lower precision than the other methods, specially "SNR-based Switching DNN" and "SNR-based Switching Staggered DNN". It was verified that, specially when $K = 3$, "Neighbors Average"

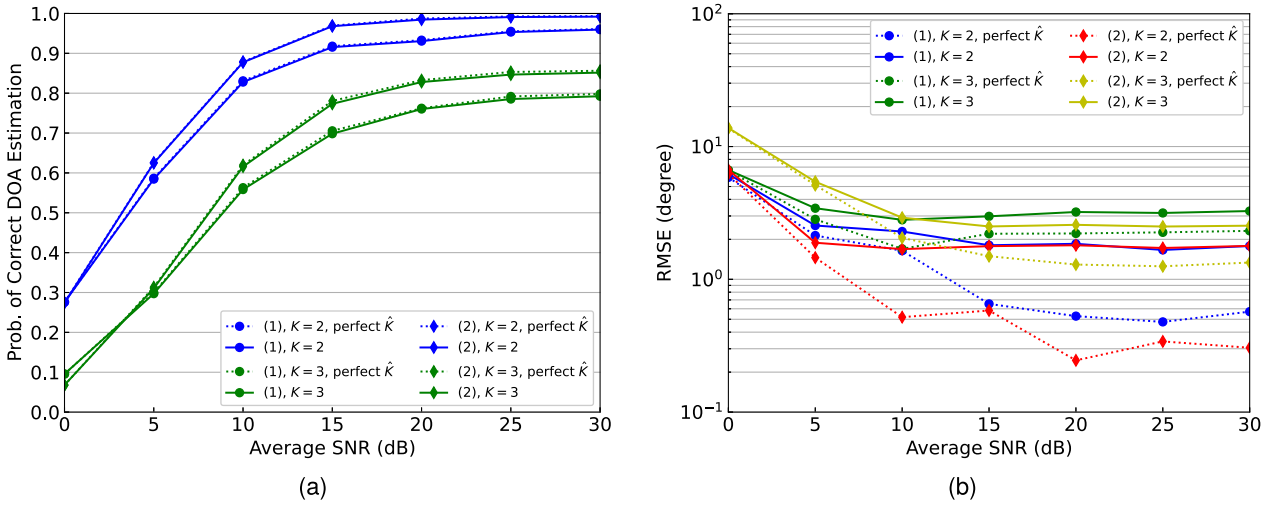

Fig. 11 Proposed system performance comparison when source number estimation is perfect (perfect $\hat{K}$) and not perfect, and when SNR-based (1) Switching DNN or (2) Switching Staggered DNNs are used as spectrum estimation techniques. SNR estimation is done with the regression-based method. (a) Probability of correct DOA estimation. (b) RMSE.

paired with "SNR-based Switching Staggered DNN" is very accurate in detecting DOA. Nevertheless, comparing the $K = 3$ case with $K = 2$, estimation precision is still largely lower. At this configuration of number of ULA elements $L = 5$ and of sources $K = 3$, DOA estimation becomes more difficult not only for root-MUSIC, but also for the proposed DNN solutions. Therefore, it is an urgent issue to develop new strategies to enhance the estimation performance at such configuration before we deploy the proposed techniques at environments with more antenna elements and/or radio wave sources.

7.4 Performance of Proposed End-to-End System

Finally we converge all the previous discussion to analyze the proposed end-to-end DOA system. For the computer simulations, we consider the following, where DOA estimation is performed with the angular spectrum grid estimator and DOA detector:

- DOA detector: "Neighbors Average" (Sect. 4),
- Angular spectrum grid estimator: "SNR-based Switching DNN" and "SNR-based Switching Staggered DNN", where SNR estimation is done with the regression-based method (Sect. 5),
- Source number estimator: DNN-based (Sect. 6).

All the training, validation, and test datasets for the corresponding models are generated in the same fashion as it has been described within this section. All DNNs and regression model have been trained offline prior to testing following the same parameters discussed in the corresponding sections. Here, we analyze the effect of perfect and imperfect source number estimators on the proposed system performance, as it is shown in Fig. 11. While RMSE degradation is evident from Fig. 11(b) even when the achieved source number estimation accuracy was over 99% (Sect. 6), the success rate remains practically unchanged (see Fig. 11(a)). We can conclude that only very few source number estimation errors are enough to severely degrade the RMSE performance. On the other hand, success rate is greatly robust to both source number and SNR estimation errors. For this reason, it is necessary to develop strategies capable of curbing this non-desirable influence from incorrect source number prediction.

8. Discussion on Regularized Loss Function

From some DNN output samples we observe that many bins unrelated to those corresponding to true DOAs end up being excited. These might in turn provoke incorrect DOA detection, specially when 5 ULA elements and 3 emitting sources is assumed. Noting the sparseness in the DNN output and taking the results from compressed sensing approaches as inspiration, here we verify the effectiveness of adding a regularization term, l_p-norm, to the MSE loss function. It is expected that, by doing so, spurious bins might be suppressed, and thus the DNN output spectrum might become more sparse and cleaner for DOA detection algorithms to operate.

Let $\{\mathbf{t}_i\}_{i=1}^{N_{\text{batch}}}$ be a batch with N_{batch} label samples, where each sample $\mathbf{t}_i \in \mathbb{R}^{U\times 1}$ and U is the number of units in the output layer (for instance, $U = 121$ in case of DNN-A). Let $\{\mathbf{v}_i\}_{i=1}^{N_{\text{batch}}}$ be the N_{batch} outputs from the DNN after forward computation. After adding the l_p-norm term, the regularized MSE loss function $\mathcal{L}$ to be minimized can be written as:

$$\mathcal{L} = \frac{1}{N_{\text{batch}}} \sum_{i=1}^{N_{\text{batch}}} \mathcal{L}_i, \tag{11}$$

$$\mathcal{L}_i = \frac{1}{U} \sum_{j=1}^{U} (v_{i,j} - t_{i,j})^2 + a \left(\sum_{j=1}^{U} v_{i,j}^p \right)^{1/p}, \tag{12}$$

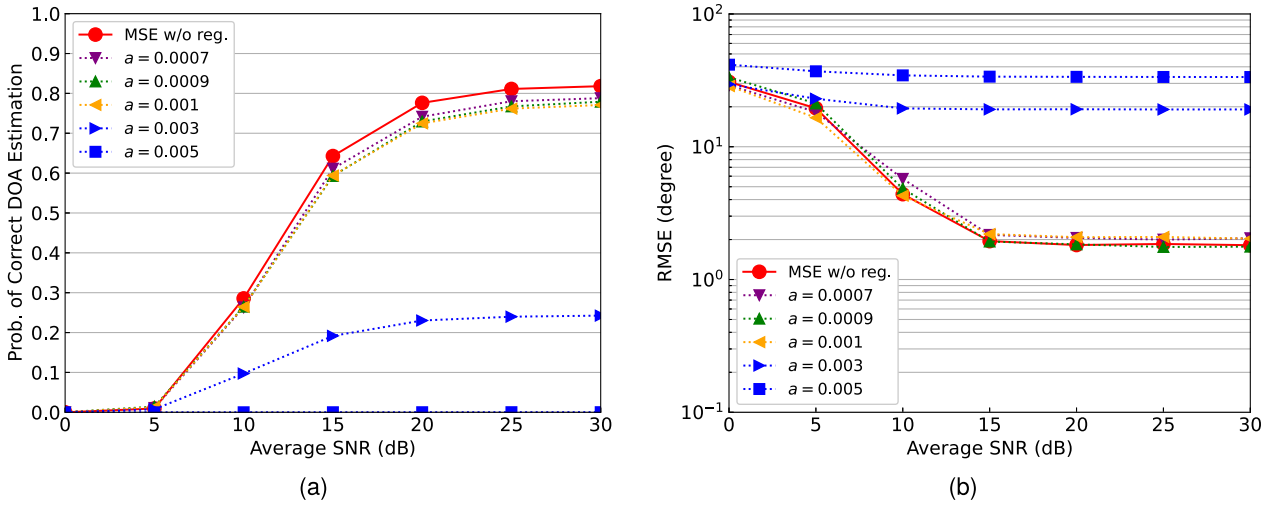

Fig. 12 Performance analysis of the DOA estimator when the MSE loss is regularized by an l_p-norm term, for the case $p = 0.95$, and varying scaling factor a. Comparison is also made with the case when no regularization term is added. (a) Probability of correct DOA estimation. (b) RMSE.

where $\mathcal{L}_i$ is the proposed regularized loss calculated for the ith sample in the batch, $t_{i,j}$ and $v_{i,j}$ are the jth unit of the label and output, respectively, in the ith batch sample, a is the scaling factor and p is the norm value, which satisfies $0 < p < 1$. However, due to its non-differentiability around the origin when $p \leq 1$, here a smooth approximation suggested in [6] is used:

$$a\left(\sum_{j=1}^{U} v_{i,j}^{p}\right)^{1/p} \approx a\left[\sum_{j=1}^{U}(v_{i,j}^{2}+\epsilon)^{p/2}\right]^{1/p}, \tag{13}$$

where ϵ is a very small value. For this study we have only considered $p = 0.95$ and $\epsilon = 1.0 \times 10^{-7}$ during simulation trials. The number of epochs was raised from 300 (Table 3) to 1,000, since the time required for training is longer with the addition of the l_p-norm. All other parameters are kept unchanged. Results of the performance analysis of the proposed approach can be seen in Fig. 12, where the number of epochs for the DNN without l_p-norm was also raised to 1,000 for fair comparison. In Fig. 13, we show two samples of the DNN output when the l_p-norm is and is not included in the loss calculation. Both DNN output samples were calculated under the same test data.

When a is larger than 0.003, there is a noticeable DOA detection accuracy degradation. It is believed that a too large l_p-norm added to the MSE masks the gradient computation done during backpropagation, which results in very poor DNN model weights. From Fig. 12(a), when $a = 0.0007$ the probability of correct DOA estimation only degrades a little compared to the case without regularization. On the other hand, from Fig. 12(b), subtle RMSE improvement can be verified when $a = 0.0009$, surpassing the curve corresponding to no regularization when the SNR is 25 dB and 30 dB.

Although little improvement can be seen from Fig. 12, the effect of producing a more sparse DNN output with the

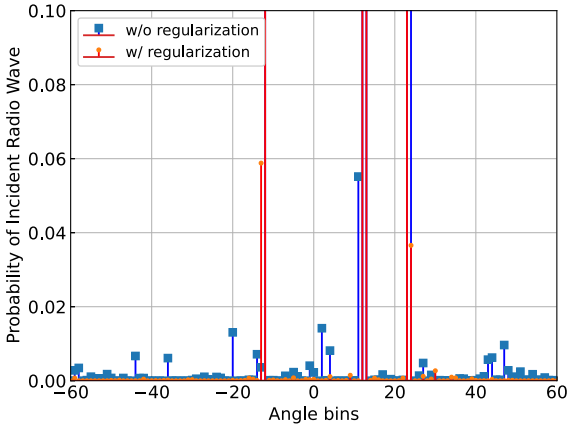

Fig. 13 Comparison of the DNN output angular spectrum obtained by a DNN trained with and without the regularization l_p-norm, when $p = 0.95$ and $a = 0.0009$. For better visualization, this graph is plotted until the probability of success of 0.10. Successful DOA detection is achieved in both cases.

l_p-norm regularization can be quickly observed in Fig. 13. There it is readily visible how well spurious bins have been suppressed by means of a technique used in conjunction with deep learning methods (backpropagation) even if it is primarily used in the context of compressed sensing. We believe that this result can be beneficial especially for the case of larger values of source number K and of narrowly incident waves. It is our future goal of further investigating the usage of the l_p-norm at these other model assumptions.

9. Final Remarks

In this paper, we presented a new end-to-end DOA estimation system consisting of three modules: source number estimator, angular spectrum grid estimator and DOA detector. Two new performance enhancement techniques for spectrum estimation, which rely on SNR estimation, were also

described. We designed two different approaches for SNR estimation, yet it was verified that the DOA detection performance metrics remained virtually unchanged for either of them, even when perfect SNR prediction had been assumed. A DNN with simple architecture specific for source number estimation, which achieved great prediction performance, was designed. A new DOA detection algorithm more precise in predicting DOA values from the DNN output angular spectrum grid in comparison with our previous method was developed. We verified that one of the proposed enhancement techniques, "SNR-based Switching Staggered DNN", had resulted in great estimation performance even compared to the traditional super-resolution root-MUSIC regarding the success rate metric for the case of two radio wave sources. On the other hand, for the case of three sources, not fully satisfactory results were obtained. Consequently, developing new approaches capable of raising our DOA estimator accuracy is our next goal for future works.

We can list the following tasks that need attention: verification of different DNN architectures and designs, such as using the binary cross-entropy as the loss function; development of backup strategies to avoid RMSE accuracy decline when the source number estimator fails. It is also an urgent matter to validate our datasets by means of, for instance, K-fold, in order to guarantee no overlapping between the training, validation, and test datasets.

References

[1] National Institute of Information and Communications Technology (NICT), Beyond 5G/6G White Paper, June 2022.
[2] R.O. Schmidt, "Multiple emitter location and signal parameter estimation," IEEE Trans. Antennas Propag., vol.AP-34, no.3, pp.276–280, March 1986, DOI: 10.1109/TAP.1986.1143830.
[3] B.D. Rao and K.V. S. Hari, "Performance analysis of root-MUSIC," IEEE Trans. Acoust., Speech, Signal Process., vol.37, no.12, pp.1939–1949, Dec. 1989, DOI: 10.1109/29.45540.
[4] K. Hayashi, M. Nagahara, and T. Tanaka, "A user's guide to compressed sensing for communications systems," IEICE Trans. Commun., vol.E96-B, no.3, pp.685–712, March 2013, DOI: 10.1587/transcom.E96.B.685.
[5] T. Nishimura, Y. Ogawa, T. Ohgane, and J. Hagiwara, "Radio techniques incorporating sparse modeling," IEICE Trans. Fundamentals, vol.E104-A, no.3, pp.591–603, March 2021, DOI: 10.1587/transfun.2020EAI0001.
[6] M. Çetin, D.M. Malioutov, and A.S. Willsky, "A variational technique for source localization based on a sparse signal reconstruction perspective," Proc. IEEE ICASSP 2002, pp.III-2965–III-2968, May 2002, DOI: 10.1109/ICASSP.2002.5745271.
[7] T. O'Shea and J. Hoydis, "An introduction to deep learning for the physical layer," IEEE Trans. Cogn. Commun. Netw., vol.3, no.4, pp.563–575, Dec. 2017, DOI: 10.1109/TCCN.2017.2758370.
[8] H. Huang, J. Yang, H. Huang, Y. Song, and G. Gui, "Deep learning for super-resolution channel estimation and DOA estimation based massive MIMO system," IEEE Trans. Veh. Technol., vol.67, no.9, pp.8549–8560, Sept. 2018, DOI: 10.1109/TVT.2018.2851783.
[9] M. Chen, Y. Gong, and X. Mao, "Deep neural network for estimation of direction of arrival with antenna array," IEEE Access, vol.8, pp.140688–140698, Aug. 2020, DOI: 10.1109/ACCESS.2020.3012582.
[10] D. Hu, Y. Zhang, L. He, and J. Wu, "Low-complexity deep-learning-based DOA estimation for hybrid massive MIMO systems with uniform circular arrays," IEEE Wireless Commun. Lett., vol.9, no.1, pp.83–86, Jan. 2020, DOI: 10.1109/LWC.2019.2942595.
[11] Z.-M. Liu, C. Zhang, and P.S. Yu, "Direction-of-arrival estimation based on deep neural networks with robustness to array imperfections," IEEE Trans. Antennas Propag., vol.66, no.12, pp.7315–7327, Dec. 2018, DOI: 10.1109/TAP.2018.2874430.
[12] S. Zhang, S. Zhang, T. Huang, and W. Gao, "Speech emotion recognition using deep convolutional neural network and discriminant temporal pyramid matching," IEEE Trans. Multimedia, vol.20, no.6, pp.1576–1590, June 2018, DOI: 10.1109/TMM.2017.2766843.
[13] G.W. Stimson, Introduction to Airborne Radar, 2nd ed., p.101, p.183, SciTech Publishing, Mendham, NJ, US, 1998.
[14] S. Ju, Y. Xing, O. Kanhere, and T.S. Rappaport, "Millimeter wave and sub-terahertz spatial statistical channel model for an indoor office building," IEEE J. Sel. Areas Commun., vol.39, no.6, pp.1561–1575, June 2021, DOI: 10.1109/JSAC.2021.3071844.
[15] M. Abadi, A. Agarwal, P. Barham, E. Brevdo, Z. Chen, C. Citro, G.S. Corrado, A. Davis, J. Dean, M. Devin, S. Ghemawat, I. Goodfellow, A. Harp, G. Irving, M. Isard, R. Jozefowicz, Y. Jia, L. Kaiser, M. Kudlur, J. Levenberg, D. Mané, M. Schuster, R. Monga, S. Moore, D. Murray, C. Olah, J. Shlens, B. Steiner, I. Sutskever, K. Talwar, P. Tucker, V. Vanhoucke, V. Vasudevan, F. Viégas, O. Vinyals, P. Warden, M. Wattenberg, M. Wicke, Y. Yu, and X. Zheng, "TensorFlow: large-scale machine learning on heterogeneous systems," Software available from tensorflow.org, 2015.
[16] Y. Kase, T. Nishimura, T. Ohgane, Y. Ogawa, D. Kitayama, and Y. Kishiyama, "Fundamental trial on DOA estimation with deep learning," IEICE Trans. Commun., vol.E103-B, no.10, pp.1127–1135, Oct. 2020, DOI: 10.1587/transcom.2019EBP3260.
[17] Y. Kase, T. Nishimura, T. Ohgane, Y. Ogawa, T. Sato, and Y. Kishiyama, "Accuracy improvement in DOA estimation with deep learning," IEICE Trans. Commun., vol.E105-B, no.5, pp. 588–599, May 2022, DOI: 10.1587/transcom.2021EBT0001.
[18] D.A. Ando, T. Nishimura, T. Sato, T. Ohgane, Y. Ogawa, and J. Hagiwara, "A proposal of an end-to-end DoA estimation system aided by deep learning," WPMC 2022, pp.98–103, Oct. 2022, DOI: 10.1109/WPMC55625.2022.10014749.
[19] G. James, D. Witten, T. Hastie, and R. Tibshirani, An Introduction to Statistical Learning with Applications in R, Springer New York, 2013.
[20] R.T. Nakatsu, "An evaluation of four resampling methods used in machine learning classification," IEEE Intell. Syst., vol.36, no.3, pp.51–57, June 2021, DOI: 10.1109/MIS.2020.2978066.
[21] S. Ioffe and C. Szegedy, "Batch normalization: Accelerating deep network training by reducing internal covariate shift," arXiv:1502.03167v3, March 2015.
[22] D.P. Kingma and J.L. Ba, "Adam: A method for stochastic optimization," arXiv:1412.6980v9, Jan. 2017.

Daniel Akira Ando received the B.E. degree in communication networks engineering from University of Brasilia, Brazil, in 2018 and the M.E. degree in media networks engineering from Hokkaido University, Japan, in 2021. He is currently pursuing the Ph.D. degree at Hokkaido University, Japan. His research interests are in MIMO signal processing for wireless communications. He received the IEICE RCS Young Researcher Award in 2020.

Yuya Kase received the B.E. degree in electrical and electronic engineering from National Institute of Technology, Asahikawa College, Asahikawa, Japan, in 2017 and the M.E. degree in the field of media and network technologies and the Ph.D. degree in Engineering from Hokkaido University, Sapporo, Japan, in 2019 and 2022, respectively. His interests are in the application of deep learning in the field of DOA estimation and mobile communications.

Toshihiko Nishimura received the B.S. and M.S. degrees in physics and Ph.D. degree in electronics engineering from Hokkaido University, Sapporo, Japan, in 1992, 1994, and 1997, respectively. Since 1998, he has been with Hokkaido University, where he is currently a Professor. His current research interests are in MIMO systems using smart antenna techniques. He received the Young Researchers' Award of IEICE in 2000, the Best Paper Award from IEICE in 2007, and TELECOM System Technology Award from the Telecommunications Advancement Foundation of Japan in 2008, the best magazine paper award from IEICE Communications Society in 2011, and the Best Tutorial Paper Award from the IEICE Communications Society in 2018. He is a member of the IEEE.

Takanori Sato was born in Hokkaido, Japan, in 1992. He received his Ph.D. degree in the field of media and network technologies from Hokkaido University, Japan, in 2018. He was a Research Fellow of Japan Society for the Promotion of Science (JSPS) from 2017 to 2019. In 2019, he moved to University of Hyogo as an assistant professor. He is currently an associate professor in Hokkaido University. His research interests include the theoretical and numerical studies of optical fibers and photonic circuits using the coupled mode theory and the finite element method. He is a member of the Japan Society of Applied Physics (JSAP), Institute of Electrical and Electronics Engineers (IEEE), and the Optical Society of America (OSA).

Takeo Ohgane received the B.E., M.E., and Ph.D. degrees in electronics engineering from Hokkaido University, Sapporo, Japan, in 1984, 1986, and 1994, respectively. From 1986 to 1992, he was with Communications Research Laboratory, Ministry of Posts and Telecommunications. From 1992 to 1995, he was on assignment at ATR Optical and Radio Communications Research Laboratory. Since 1995, he has been with Hokkaido University, where he is currently a Professor. During 2005–2006, he was at Centre for Communications Research, University of Bristol, U.K., as a Visiting Fellow. His research interests are in MIMO signal processing for wireless communications. He received the IEEE AP-S Tokyo Chapter Young Engineer Award in 1993, the Young Researchers' Award of IEICE in 1990, the Best Paper Award from IEICE in 2007, TELECOM System Technology Award from the Telecommunications Advancement Foundation of Japan in 2008, the Best Magazine Paper Award from IEICE Communications Society in 2011, and the Best Tutorial Paper Award from IEICE Communications Society in 2018. He is a member of the IEEE.

Yasutaka Ogawa received the B.E., M.E., and Ph.D. degrees from Hokkaido University, Sapporo, Japan, in 1973, 1975, and 1978, respectively. Since 1979, he has been with Hokkaido University, where he is currently a Professor Emeritus. During 1992–1993, he was with ElectroScience Laboratory, the Ohio State University, as a Visiting Scholar, on leave from Hokkaido University. His professional expertise encompasses super-resolution estimation techniques, applications of adaptive antennas for mobile communication, multiple-input multiple-output (MIMO) techniques, and measurement techniques. He proposed a basic and important technique for time-domain super-resolution estimation for electromagnetic wave measurement such as antenna gain measurement, scattering/diffraction measurement, and radar imaging. Also, his expertise and commitment to advancing the development of adaptive antennas contributed to the realization of space division multiple accesses (SDMA) in the Personal Handy-phone System (PHS). He received the Yasujiro Niwa Outstanding Paper Award in 1978, the Young Researchers' Award of IEICE in 1982, the Best Paper Award from IEICE in 2007, TELECOM system technology award from the Telecommunications Advancement Foundation of Japan in 2008, the Best Magazine Paper Award from IEICE Communications Society in 2011, the Achievement Award from IEICE in 2014, and the Best Tutorial Paper Award from IEICE Communications Society in 2018. He also received the Hokkaido University Commendation for excellent teaching in 2012. He is a Life Fellow of the IEEE.

Junichiro Hagiwara received the B.E., M.E., and Ph.D. degrees from Hokkaido University, Sapporo, Japan, in 1990, 1992, and 2016, respectively. He joined the Nippon Telegraph and Telephone Corporation in April 1992 and transferred to NTT Mobile Communications Network, Inc. (currently NTT DOCOMO, INC.) in July 1992. Later, he became involved in the research and development of mobile communication systems. His current research interests are in the application of stochastic theory to the communication domain. He is currently a visiting professor at Hokkaido University